Available online at www.sciencedirect.com
SCIENCE DIRECT®
International Journal of Pharmaceutics 295 (2005) 269–281
international journal of pharmaceutics
www.elsevier.com/locate/ijpharm

Pharmaceutical Nanotechnology

Effect of nanoprecipitation on the physicochemical properties of low molecular weight poly(L-lactic acid) nanoparticles loaded with salbutamol sulphate and beclomethasone dipropionate

S. Hyvönen*, L. Peltonen, M. Karjalainen, J. Hirvonen

Division of Pharmaceutical Technology, Faculty of Pharmacy, University of Helsinki, P.O. Box 56, FIN-00014, Finland

Received 9 January 2005; received in revised form 15 February 2005; accepted 27 February 2005

Abstract

A modified nanoprecipitation (interfacial polymer deposition following solvent displacement) method was used to produce nanoparticles from low molecular weight poly(L-lactic acid). Model drugs, either salbutamol sulphate or beclomethasone dipropionate, were encapsulated in the particles. The influence of the preparation method on the physicochemical state of the polymer and the drugs as well as on the drug–polymer interactions were studied by electron microscopy, X-ray diffractometry, thermal analysis and infrared spectroscopy. Nanoprecipitation lowered the crystallinity of the PLA polymer. The crystallinity of the polymer was higher in the particles containing salbutamol sulphate then those containing beclomethasone dipropionate. The crystal form of beclomethasone dipropionate was changed from an anhydrate to a monohydrate as a result of nanoprecipitation. Although changes in the crystallinity of the polymer and the model drugs were seen, no clear interactions between the polymer and the drug were detected.

Keywords: Nanoprecipitation; Poly(L-lactic acid); Salbutamol sulphate; Beclomethasone dipropionate; Physicochemical characterization

1. Introduction

When nanoparticles are produced by a method which involves solvation of the polymer and the drug and, further, evaporation of the solvent leading to precipitation, the state of the drug and the polymer may vary from crystalline to amorphous. The drug can be present as a solid solution (dissolved) or it may form either a molecular or a crystalline dispersion among the polymeric matrix (Dubernet, 1995). Besides, the state of the drug can be a combination of different possibilities: it can be partly solubilised in the polymer and partly deposited in the matrix as both amorphous and crystalline domains (Ramtoola et al., 1991; Wang et al., 2004). For example, the rate of increase in viscosity of the hosting polymer (transformation from amorphous to crystalline) during the evaporation of the solvent can determine, whether the drug reaches

* Corresponding author. Tel.: +358 919 159 306; fax: +358 919 159 144.
E-mail address: samuli.hyvonen@helsinki.fi (S. Hyvönen).

0378-5173/$ – see front matter © 2005 Elsevier B.V. All rights reserved.
doi:10.1016/j.ijpharm.2005.02.026

Table 1
Interaction studies of poly(L-lactides) and drugs when both the polymer and the drug are in dissolved state during the particle preparation process

Drug	PLA M_W (g/mol)	Conclusion	Reference
Papaverine hydrochloride	4000; 8000	The drug is dissolved in polymer matrix at 10% loading.	Miyajima et al. (1997)
Sodium diclofenac	2500[a]	Cold-crystallization of the drug is delayed during the solvent evaporation leading to an amorphous form of the drug.	Lin et al. (2000)
Loperamide	110,100	The drug is present in the nanoparticles as an amorphous material.	Ueda and Kreuter (1997)
Amine drugs	100,000	Amine drugs reduce T_g of the polymer.	Cha and Pitt (1989)
Progesterone	10,000	The drug is molecularly dispersed in the polymeric microparticles.	Izumikawa et al. (1991)
Budesonide	100,000	The drug is amorphous in the polymeric microparticles (due to the supercritical fluid precipitation technique).	Martin et al. (2002)
Beclomethasone dipropionate, nedocromil sodium	2000	No interactions between the drugs and the polymer in the microspheres.	El-Baseir et al. (1997)
Paclitaxel	100,000	Plasticizing effect of the drug became more evident, when the size of microspheres were larger.	Liggins and Burt (2004a)
Paclitaxel	A blend of 60% 1000 and 40% 100,000	The drug was miscible in microparticles by increasing T_g, T_c and decreasing T_m of the polymer blend.	Liggins and Burt (2004b)

[a] Molecular weight is reported as a number average molar mass (M_N).

its crystalline state or remains molecularly dispersed in the polymer (Benoit et al., 1986). Correspondingly, if the drug remains dissolved in the polymer matrix, the polymer may interact with the drug (Jenquin and McGinity, 1994). As a consequence, the state of the drug and the hosting polymer play an important role in determining the essential properties of the system, including entrapment and release of the drug. In general, the interactions of drugs and polymers in nanoparticulate systems are not as widely studied as in microparticle systems. Studies of such interactions in drug-poly(L-lactic acid) systems are listed in Table 1.

In this study, properties and possible physicochemical interactions of two different model drugs, salbutamol sulphate and beclomethasone dipropionate, with a semicrystalline polymer, low molecular weight poly(L-lactic acid) (M_W 2000 g/mol), were studied. Henceforth poly(L-lactic acid), salbutamol sulphate and beclomethasone dipropionate are referred to as PLA, SS and BDP, respectively. Drug–PLA samples were characterized by thermoanalysis, X-ray diffractometry, infrared spectroscopy and electron microscopy. The model drugs were selected to represent different properties: SS is a freely water-soluble drug and it carries a positive charge when dissolved. BDP is a non-ionized drug that is practically insoluble in water. Low M_W polylactides open up possibilities to drug delivery, where the polymeric vehicle is designed to degrade fast in the body, e.g., for pulmonary delivery. Production of particles from low M_W PLA is more difficult compared to high molecular weight polylactides, for several reasons. Low M_W PLA has higher solubility (as compared to the higher M_W PLA) in some commonly used organic solvents and therefore precipitation of the polymer occurs more slowly and more solvent has to be removed to precipitate the polymer during the preparation (Bodmeier et al., 1989; Mehta et al., 1996). Low M_W PLA is also more sticky than polymers with higher M_W, which causes aggregation tendency (Wichert and Rohdewald, 1990). Additionally, the lower the M_W of the PLA, the higher is the water-soluble fraction of the polymer. For example, Liggins and Burt (2001) found out that approximately one third of 1000 g/mol PLA was soluble in water. The particle yield has also been reported to decrease as the water-soluble fraction was increased (Mehta et al., 1996). The special aim of this study was to find out the effect of a nanoparticle preparation

method, modified nanoprecipitation, on the behaviour and properties of the drugs and the polymer.

2. Materials and methods

2.1. Materials

Poly(L-lactic acid) (ICN Biomedicals, Inc., Aurora, OH, USA) of molecular weight 2000 g/mol formed the nanoparticulate matrix. Model drugs studied were salbutamol sulphate (a donation from Orion Pharma, Espoo, Finland) and (anhydrous) beclomethasone dipropionate (Sigma Chemical Co., St. Louis, MO, USA). Other excipients used were dichloromethane (Riedel-de Haën, Seelze, Germany), ethanol (96%, v/v) (Primalco, Rajamäki, Finland) and propylene glycol (YA Kemia, Helsinki, Finland). Water was ultrapurified Millipore water (Millipore, Molsheim, France).

2.2. Preparation of formulations

Three different types of formulations were prepared for the analysis: formulations without the drugs (empty PLA particles), SS containing formulations and BDP containing formulations. All the formulations were prepared by a modified nanoprecipitation method (Peltonen et al., 2002). Twenty-five milligrams of PLA and 175 mg of propylene glycol (stabilizer) were dissolved in 2 ml of dichloromethane. In the BDP containing formulations, the drug was dissolved together with the polymer and the stabilizer. In the SS containing formulations, the drug was dissolved in 0.15 ml of water, and 0.7 ml of 96% ethanol was added to act as a co-solvent. Subsequently, the polymeric solution was poured to the SS solution (formation of dispersion, the inner phase). Correspondingly, in the BDP formulations, the co-solvent and water were added to the polymer solution. Formulations without the drugs were prepared as the BDP formulations except the drug. The formed aqueous dichloromethane–ethanol dispersion was shaken manually followed by a dropwise addition to 70% (v/v) ethanol solution (5 ml, the outer phase) under mild stirring. The organic solvents were evaporated and the formulations were dried under slight vacuum at room temperature.

In a standard preparation procedure of nanoparticles, amounts of the drug and the polymer were 2.5 mg and 25 mg, respectively (1:10). For the analysis, formulations containing 5 mg (1:5) and 10 mg (1:2.5) of the drugs were also prepared according to the modified nanoprecipitation procedure above. Also physical mixtures of each drug and the PLA polymer were prepared by mixing the powders together. The drug:polymer ratio in the physical mixtures was the same as in the standard nanoparticle formulations (1:10).

2.3. Characterization of nanoparticle morphology and size

The surface morphology (roundness, formation of aggregates) and size of the nanoparticles were studied by scanning electron microscopy (SEM). A drop of particle suspension was deposited on a metal plate 5 min after preparation, let to dry and sputtered for 20 s with platinum (Agar Sputter Coater, Agar Scientific Ltd., Essex, UK) and, finally, analysed with a SEM (DSM 962, Zeiss, Jena, Germany).

2.4. XRPD experiments

X-ray diffraction patterns were measured using X-ray powder diffraction (XRPD) theta–theta diffractometer (Bruker axs D8, Karlsruhe, Germany). The XRPD experiments were performed in symmetrical reflection mode with Cu Kα radiation (1.54 Å) using Göbel Mirror bent gradient multilayer optics. The scattered intensities were measured with a scintillation counter. The angular range was from 5° to 30° with the steps of 0.1° and the measuring time was 20 s per step.

XRPD diffraction patterns were determined from the pure materials, physical mixtures and the drug–PLA formulations. The pure materials included PLA, SS and BDP powders. Nanoparticles were either empty (only PLA) or contained SS or BDP. Also the formulations containing higher amounts of the drugs (1:5 and 1:2.5) were analysed. Powder samples were analysed as such. Other samples were prepared by depositing suspensions of the formulations on silica plates after preparation, dried under slight vacuum at room temperature, and analysed as such.

2.5. XRPD data analysis

Crystallinities of the samples were estimated by fitting intensity of a crystalline component and intensity of an amorphous component to the experimental intensity curve. The crystallinity of the samples was

obtained as the ratio of the integrals of the intensities of the crystalline component and the studied sample. The intensity curve of melted PLA at 165 °C was used as the amorphous model intensity curve, and the intensity curve, where the amorphous model intensity curve had been subtracted, was used as the crystalline model intensity curve. For identification of crystal structures, diffraction patterns of SS, BDP anhydrate and BDP monohydrate were calculated based on the single crystal data taken from the Cambridge Crystallographic Data Centre (CCDC).

Contributions of each starting material to the crystallinities of the samples were estimated. They were presented as the relative amount of crystallinity of the sample. The calculation was based on the assumption that the experimental intensity curve of crystalline part of the sample is a linear combination of the intensities of crystalline parts of the starting materials. The relative amount of the structure of each starting material component was estimated by fitting the diffraction curve of the crystalline part of the component to the experimental diffraction curve of the crystalline part of the sample.

2.6. DSC experiments

Thermal behaviour of the materials was determined using DSC822^e differential scanning calorimeter (Mettler Toledo, Columbus, USA). Samples were heated at the rate of 10 °C/min. Results were analysed with STAR^e software (Mettler Toledo).

Samples for the DSC experiments included the same compositions as the XRPD samples. Suspensions of the formulations were let to dry, powdered, and weighted (2–4 mg) to aluminium pans and crimped by aluminium caps with a pinhole. All the samples were heated first from 30 °C to 200–220 °C (depending on the melting temperature of the sample) and thermograms were registered (1st scan). The samples were held at the end temperature for 2 min, and after that cooled to −10 °C at the rate of 20 °C/min. After this cooling the samples were re-heated and the new thermograms were registered (2nd scan).

2.7. FTIR experiments

IR spectra were registered with Spectrum One FTIR Spectrometer equipped with Universal ATR Sampling Accessory (Perkin-Elmer, Boston, USA).

Samples for the FTIR experiments were of the same compositions as the DSC samples (except the physical mixtures). Small amounts (2–3 mg) of the powders or the dried and powdered samples were used for the analysis.

3. Results and discussion

3.1. Morphology and size of nanoparticles

The nanoprecipitation method is very sensitive to changes in composition (Peltonen et al., 2002, 2003). Among the tested compositions, round and smooth "high-quality" nanoparticles were formed when the model drugs were not present and with the 1:10 drug loadings. Higher drug loadings (1:5; 1:2.5) were also tested to achieve a better understanding about the effect of each drug on the polymer as well as on the state of the drug during the nanoprecipitation process. SEM images of empty PLA nanoparticles, SS containing (1:10) nanoparticles and BDP containing (1:10) nanoparticles are presented in Fig. 1. The size distribution of SS–PLA particles was settled mainly in the range of 500–900 nm, while the diameters of the empty particles and the BDP–PLA particles were smaller, 300–500 nm.

3.2. XRPD experiments

The diffraction pattern of PLA included reflections at about 14.8°, 16.7°, 19.1° and 22.4° (2θ) corresponding to Bragg distances of 6.0 Å, 5.3 Å, 4.6 Å and 4.0 Å, respectively. The crystallinity of PLA was 59% indicating its semicrystalline nature (Table 2). The crystallinity of the polymer decreased to 39% after nanoprecipitation (empty particles), which was expected due to the polymer precipitation caused by the rapid diffusion of dichloromethane to the outer phase. Correspondingly, it has been shown that fast evaporation of polymer-dissolving organic solvent inhibits crystallization of the polymer, because the polymer network has less time to organize (Izumikawa et al., 1991). It should be noted that the calculated crystallinity percentages are not exact values, but estimations based on the model (see Section 2.5). However, they provide comparable crystallinity values.

Fig. 2 presents the measured XRPD diffraction patterns of PLA, empty particles, SS, physical mixture of

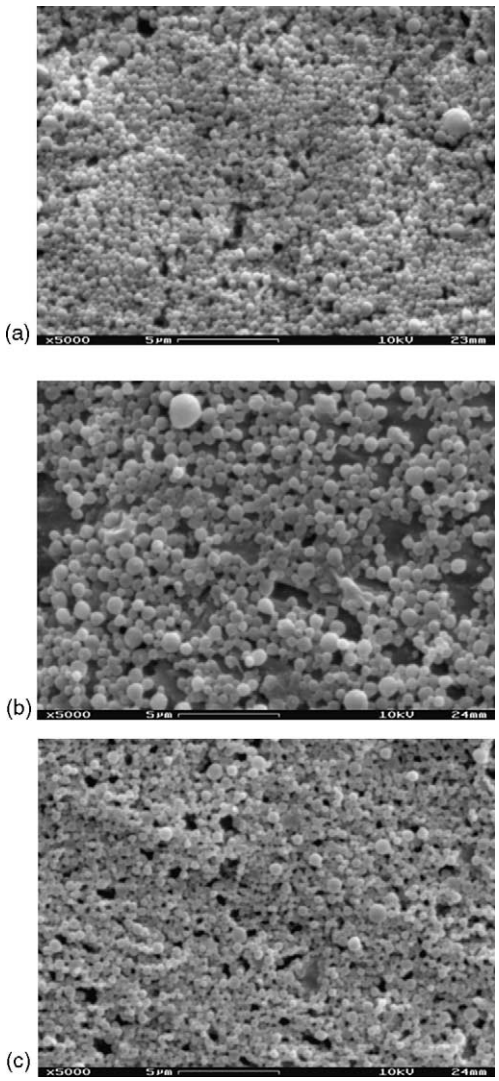

Fig. 1. SEM images of (a) empty PLA nanoparticles; (b) nanoparticles containing (1:10) SS; (c) nanoparticles containing (1:10) BDP.

SS and PLA, and the three different formulations of SS–PLA. The diffraction pattern of SS powder showed strong reflections of crystalline SS. The calculated crystallinity of SS was 81% (Table 2). The overall crystallinity of the SS–PLA physical mixture was 62%. Crystal structures of the starting materials were seen clearly in the diffraction pattern of the physical mixture. The relative amounts of crystal structures were 25% for SS and 75% for PLA. Crystal structure of SS could also be detected in all the SS–PLA samples

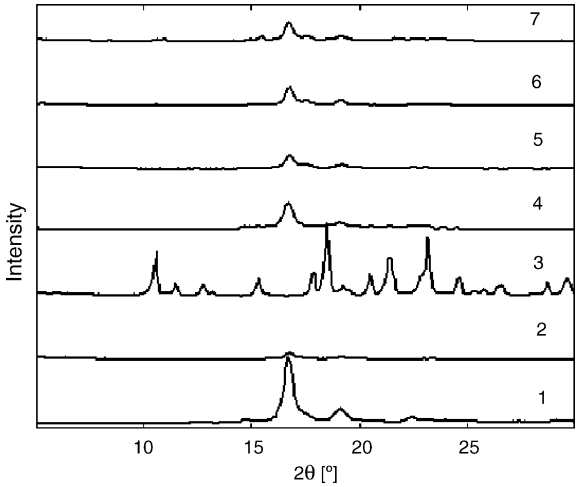

Fig. 2. X-ray diffractograms of: (1) PLA; (2) empty PLA nanoparticles; (3) SS; (4) physical mixture of SS and PLA; (5) SS:PLA 1:10 nanoparticles; (6) SS:PLA 1:5 nanoparticles; (7) SS:PLA 1:2.5 nanoparticles.

(Fig. 2 and Table 2). Thus, at least part of the drug remained crystalline also after the nanoprecipitation. The locations of the diffraction peaks of the components (SS and PLA) did not change, which indicates that the crystalline portion of both the components maintained its structure.

Interestingly, although the amount of the more crystalline material SS was increased with respect to the polymer, the relative amount of the crystalline PLA remained high (Table 2). The nanoprecipitation was expected to lower the crystallinity of the polymer (as seen from the empty particles). If the SS–PLA ratios used in preparation (1:10, 1:5 and 1:2.5) are transformed to crystallinity proportions according to the measured crystallinities of the starting materials, SS (81%) and PLA (59%), the obtained values can be compared to the corresponding values after nanoparticle preparation. The obtained crystallinity proportions for the formulations were SS 12% and PLA 88% (1:10), SS 22% and PLA 78% (1:5), and SS 35% and PLA 65% (1:2.5). The corresponding relative crystallinities of PLA after the preparation process were higher (except with the smallest amount of SS) (Table 2). Thus, it seems obvious that the presence of SS enhanced the crystallinity of PLA.

Fig. 3 presents the measured XRPD diffraction patterns of PLA, empty PLA nanoparticles, BDP,

Table 2
The average crystallinity values of the formulations and the contributions of the starting materials to the crystallinity

Sample	Crystallinity (%)	Relative amount of crystalline part (%)		
		Salbutamol sulphate	Beclomethasone dipropionate	PLA
Salbutamol sulphate	81	100	–	–
Beclomethasone dipropionate	83	–	100	–
PLA powder	59	–	–	100
Empty PLA nanoparticles	39	–	–	100
Physical mixture of SS and PLA	62	25	–	75
Physical mixture of BDP and PLA	67	–	11	89
SS:PLA 1:10	54	14	–	86
SS:PLA 1:5	59	16	–	84
SS:PLA 1:2.5	61	22	–	78
BDP:PLA 1:10	44	–	21 (a:17; m:83)	79
BDP:PLA 1:5	55	–	29 (a:8; m:92)	71
BDP:PLA 1:2.5	55	–	44 (a:6; m:94)	56

In the BDP–PLA samples, relative percentages of BDP anhydrate and BDP monohydrate in the sample are indicated as 'a', BDP anhydrate; 'm', BDP monohydrate.

physical mixture of BDP and PLA, and the three formulations of BDP–PLA. The diffraction pattern of BDP powder included strong reflections indicating the crystalline structure of the anhydrous BDP. The calculation gave also a very high value to the crystallinity of BDP (Table 2). In the physical mixture, both BDP (anhydrate) and PLA reflections were present.

BDP is reported to form solvates with a variety of solvents, e.g., with alcohols (Jinks, 1989), and halogenated hydrocarbons (Cook and Hunt, 1982). Monohydrate of BDP can be prepared for example by dissolving the anhydrous drug in ethanol and, subsequently, the addition of water crystallizes it as the monohydrate (Nachiengtung, 1997). The monohydrate form is more stable than the anhydrous form (Duax et al., 1981). In the diffraction pattern of BDP–PLA samples (which had been gone through the nanoprecipitation process), new reflections could be seen (Fig. 3). These new reflections matched with the monohydrate form, and the calculations confirmed that the majority of BDP had been crystallized as the monohydrate (Table 2). The overall crystallinities of the BDP–PLA samples were slightly lower than those of the SS–PLA samples (Table 2). Also the relative BDP–PLA crystallinity values were lower than the corresponding SS–PLA values. When the BDP–PLA ratios studied were transformed to crystallinity proportions with the help of the starting material crystallinities (as with the SS–PLA formulations), the obtained values were BDP 12% and PLA 88% (1:10), BDP 22% and PLA 78% (1:5), and BDP 36% and PLA 64% (1:2.5). When compared to the relative crystallinities after nanoparticle preparation (Table 2), the PLA crystallinities after nanoprecipitation were lower. This finding was opposite to the behaviour of the SS–PLA samples. The crystallinity values of PLA obtained by these calculations could not be compared to the crystallinity of the empty particles. However, it seemed that the polymer crystallinity was higher when SS was

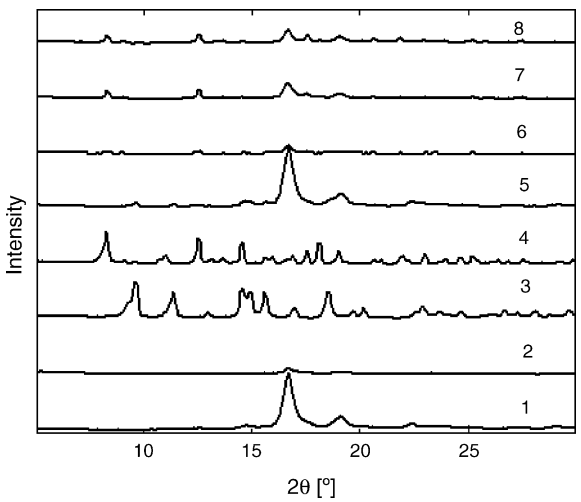

Fig. 3. X-ray diffractograms of: (1) PLA; (2) empty PLA nanoparticles; (3) BDP anhydrate; (4) BDP monohydrate; (5) physical mixture of BDP and PLA; (6) BDP:PLA 1:10 nanoparticles; (7) BDP:PLA 1:5 nanoparticles; (8) BDP:PLA 1:2.5 nanoparticles.

Table 3
Thermal properties of the starting materials and the physical mixtures

Sample	Melting temperature of the polymer (T_m) (°C)[a]	Melting temperature of the drug (T_m) (°C)[a]
PLA	152.0	–
Salbutamol sulphate	–	201.9
Beclomethasone dipropionate	–	211.5
Physical mixture of SS and PLA	152.5	204.0
Physical mixture of BDP and PLA	151.3	–

[a] Peak maximum.

present and lower (obviously closer to the crystallinity of the empty particles) when BDP was present.

3.3. DSC experiments

DSC was used in addition to XRPD to gain more information about the crystallinity and possible interactions between PLA and the drugs. Thermograms of the drug–PLA formulations, the starting materials as well as the physical mixtures of the drugs and the polymer were analysed (Table 3). The samples were first heated above the melting points of the individual components and then cooled fast to −10 °C. The idea of the fast cooling was to disturb the crystallization of PLA from the melt. As a consequence, glass transition temperatures (T_g) and cold-crystallization temperatures (T_c) of PLA were expected to become visible in the thermograms of the re-heated samples.

PLA powder and empty PLA nanoparticles exhibited melting endotherms with a peak maximum at about 152 °C. When the DSC thermograms of PLA powder and empty PLA nanoparticles were compared, a cold-crystallization exotherm at about 100 °C appeared in the thermogram of nanoparticles (Fig. 4). The exotherm indicated that nanoprecipitation lowered the degree of crystallinity of PLA, which was also seen in the XRPD results. In the heating thermograms of the melt-cooled samples of PLA and the empty PLA particles, exotherms around 80 °C could be seen. The difference of the polymer cold-crystallization exotherm temperatures between the 1st and the 2nd scan indicated that the melt-cooling additionally decreased the crystallinity of the polymer. Two-peaked melting endotherm of PLA in the heating thermograms of the melt-cooled samples seemed to be a typical behaviour of the PLA polymer (Yasuniwa et al., 2004).

The thermogram of pure SS exhibited a peak of a melting endotherm at 202 °C, which could also be

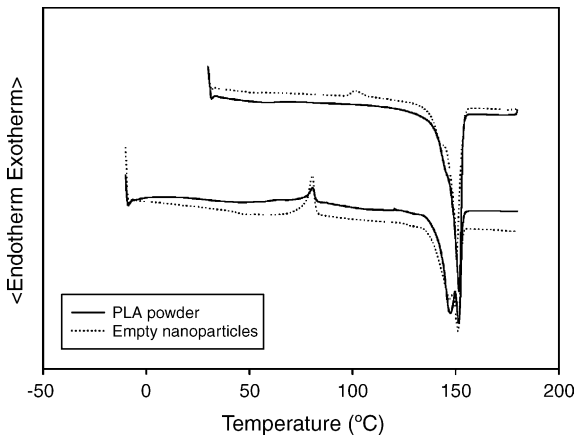

Fig. 4. DSC thermograms of the samples containing only the PLA polymer. Two thermograms above: 1st scan; two thermograms below: 2nd scan.

detected in the thermogram of the physical mixture of the drug and the polymer (Table 3), although the peak was smaller and broader. Melting point of the polymer in the physical mixture was located at the same temperature as it was in the thermogram of the pure polymer. The melting peak of SS disappeared in the nanoparticulate sample (2.5 mg of SS), but reappeared weakly in the sample containing 10 mg of SS. Similar reappearance of the drug peak with an increasing drug loading has been reported with methadone loaded poly(D,L-lactide) microspheres (Delgado et al., 1996). The disappearance of the drug-melting peak is explained by the miscibility of the drug in the polymer rather than by, e.g., transformation to an amorphous state due to the preparation technique (Jenquin and McGinity, 1994). Another explanation for the disappearance of the drug-melting peak in the nanoparticulate sample could be the low amount of the drug (2.5 mg) compared to the polymer. Nevertheless, traces of crystalline SS could be detected also from the XRPD results (Table 2).

SS is a basic drug containing a secondary amine group. When the M_W of the PLA decreases or the amount of low M_W PLA is increased in a polymer blend, the carboxylic acid content increases (Bodmeier et al., 1989; Mehta et al., 1996). Thus, low M_W PLA contains a considerable amount of carboxylic acid groups, which are located at the ends of the polymer chains. Amine drugs are reported to interact electrostatically with carboxylic acids (Borodkin and Yunker, 1970). If there was an electrostatic interaction between the SS and the carboxylic acid chain ends of the PLA, it might reduce the ability of the polymer chains to reorganize and crystallize during the evaporation phase by interrupting the intermolecular interactions of the polymer. This phenomenon is related to the decrease of T_g's observed in studies between polylactides and amines or positively charged groups, and the interaction can be detected even at low loadings of the interacting additive (Cha and Pitt, 1989; Lee et al., 2003). In this study, the DSC results showed no indications of such interactions between the polymer and SS.

The cooling rate of 20 °C/min was not fast enough to prevent crystallization of the polymer in the SS containing samples. This could be seen as exotherms in the cooling thermograms (data not shown) and as the lack of T_g's together with small-sized cold-crystallization exotherms in the 2nd scan thermograms (Fig. 5 and Table 4). The presence of SS did not change the temperatures of the cold-crystallization exotherm and the melting endotherm of PLA, when compared to the samples containing only PLA (Table 4). However, the size of the 2nd scan cold-crystallization exotherm of PLA was diminished as the amount of SS was increased in the sample (Fig. 5), as if the drug was facilitating the crystallization of the polymer during the cooling. Attempts were made to cool down the samples faster to prevent the polymer crystallization. The T_g's became visible and the cold-crystallization exotherms were larger, but the temperatures of the thermal events did not change notably compared to the pure PLA samples (data not shown). Different plasticizers are reported to promote crystallinity of poly(lactides) by enhancing the polymer chain mobility (Martin and Avérous, 2001; Ljungberg and Wesslén, 2002). The presence of SS promoted the crystallinity of PLA, which was also shown in the XRPD results. The DSC results also confirmed that the high relative amount of crystalline PLA in the samples (Table 2) was more due to the increased amount of crystalline polymer rather than SS, which could have been transformed into an amorphous form.

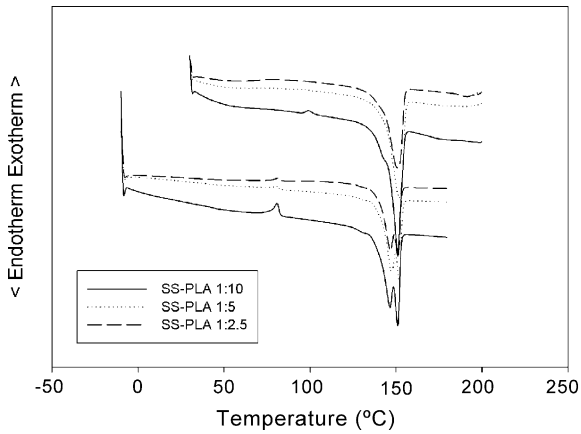

Fig. 5. DSC thermograms of the samples containing SS and PLA. Three thermograms above: 1st scan; three thermograms below: 2nd scan.

Table 4
Summary of thermal properties of PLA in the cooled and re-heated drug–PLA samples (2nd scan)

Sample	Glass transition temperature (T_g) (°C)	Cold-crystallization temperature (T_c) (°C)[a]	Melting temperature (T_m) (°C)[a]
PLA	nd[b]	80.7	151.5
Empty nanoparticles	43.9	80.5	151.1
SS:PLA, 1:10	nd[b]	80.8	150.9
SS PLA, 1:5	nd[b]	80.3	151.7
SS:PLA, 1:2.5	nd[b]	81.3	151.0
BDP:PLA, 1:10	44.8	92.2	148.1
BDP:PLA, 1:5	46.9	101.8	146.5
BDP:PLA, 1:2.5	49.8	107.9	144.2

[a] Peak maximum.
[b] Not detected.

The thermogram of pure BDP exhibited a melting endotherm peak at 212 °C. From the physical mixture, melting of the polymer (151 °C) could be detected, while the melting endotherm of the drug was absent (Table 3). Absence of this endotherm could be caused by softening and thermal degradation of the polymer melt at above 200 °C (Li et al., 1996), or the possible miscibility of BDP in the PLA at high temperatures. Melting point of the polymer in the physical mixture was located at the same temperature as in the thermogram of the pure polymer. While the XRPD diffraction patterns of the three BDP–PLA samples and the physical mixture showed the presence of crystalline BDP, the melting peak of BDP could only be detected from the thermogram of the BDP–PLA 1:2.5 sample at a slightly lower temperature (196 °C). When BDP powder was scanned by the DSC, degradation of the drug could be seen straight after the melting. Because no signs of degradation were seen in the 1st scan thermograms above the presumed melting temperature of the drug, the BDP–PLA samples were exposed to the melt-cooling and the 2nd scan.

In all the BDP containing PLA samples (except the physical mixture), a small cold-crystallization exotherm of the polymer at around 100 °C could be seen. It is a sign of the amorphous polymer. Compared to the SS–PLA samples, the structures of the BDP–PLA samples were less crystalline (Table 2). No crystallization could be seen from the cooling thermograms, unlike in the case of the SS samples, when the BDP containing samples were cooled at the rate of 20 °C/min (data not shown). Thus, the presence of BDP promoted amorphous rather than crystalline form of the polymer.

As the XRPD experiments proposed that the BDP was present as a monohydrate after nanoprecipitation, BDP monohydrate was prepared from the BDP anhydrate by the method described by Nachiengtung (1997) and scanned by the DSC. The BDP monohydrate powder showed first an increase in heat flow until 100 °C (removal of the water in the crystal structure) followed by an exothermic rise in the curve. At 133 °C, an exothermic peak could be detected. Finally, the drug melted at 211 °C. Same kind of behaviour caused by the BDP monohydrate was clearly seen in the BDP–PLA 1st scan thermograms (Fig. 6): first an increasing heat flow followed by an exotherm at 100 °C (cold-crystallization of the polymer), and then a broad exotherm before the melting of the polymer at

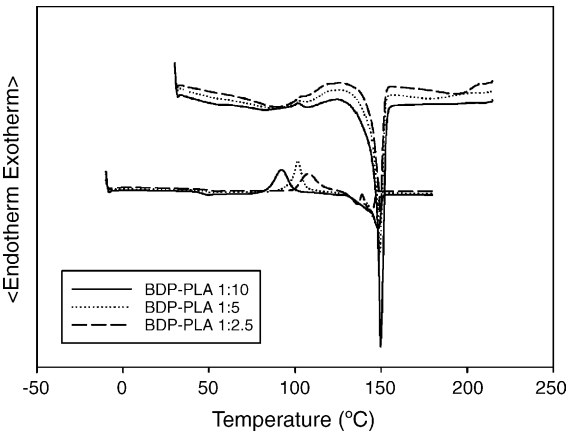

Fig. 6. DSC thermograms of the samples containing BDP and PLA. Three thermograms above: 1st scan; thee thermograms below: 2nd scan.

151 °C. When the amount of BDP in the samples was increased, the endothermic change before 100 °C and the exotherm around 130 °C became more intense. Nachiengtung explained that the (133 °C) exotherm indicated the transformation of the dehydrated monohydrate to the anhydrate form (Nachiengtung, 1997).

In the cooled and re-heated samples (2nd scan), the T_g's and the T_c's of the polymer shifted to higher temperatures as the amount of BDP was increased (Table 4, Fig. 6). It has been shown that the T_g and the T_c of an amorphous material can be raised by the addition of another amorphous compound having a higher T_g (Yoshioka et al., 1995). Amorphous BDP has a T_g around 100 °C and it crystallizes at 130–140 °C (Eerikäinen and Kauppinen, 2003). It seemed obvious that BDP was amorphous after the melt-cooling (no crystallization was detected during the cooling), and the elevation of the T_g and T_c of PLA with the increasing amounts of BDP was due to the amorphous drug. The reduction of the PLA melting temperatures with increasing drug content in the 2nd scan was a consequence of the drug acting as an "impurity". Crystallization of the amorphous BDP at around 140 °C, clearly seen in the BDP–PLA 1:2.5 sample, had also its contribution to the observed reduction in the PLA melting temperature. As no crystallization was detected during the cooling of BDP–PLA samples (after the 1st scan), a part of PLA crystallized only just during the 2nd scan, which further resulted in smaller PLA melting endotherms. The DSC results, combined with the XRPD

results, suggested that BDP was, among the polymer, mostly crystalline representing the monohydrate form and a small portion of the anhydrous form (as the original powder).

3.4. FTIR experiments

IR spectra of PLA, SS, BDP and the drug–polymer nanoprecipitated formulations were registered to elucidate, if there were any interactions between the polymer and the drugs, and to get more information about the crystal structures. Also the spectrum of the prepared BDP monohydrate was registered for comparison purposes.

A shift of the PLA carbonyl peak (~1760 cm^{-1}) to a higher wavenumber due to the weakened hydrogen bonding has been used as a proof of the transformation of the polymer from crystalline to amorphous state (Izumikawa et al., 1991). Unlike XRPD and DSC, FTIR did not reveal the decrease of crystallinity of the polymer as a consequence of nanoprecipitation. Such a shift would have probably resulted from a greater decrease of crystallinity. The characteristic peak of PLA's carbonyl bonds was located at 1757 cm^{-1}, and its place remained the same in the spectra of the PLA powder and the empty nanoparticles (Fig. 7). The PLA carbonyl peak did not change its wavenumber in any of the SS or BDP containing samples.

IR spectrum of the SS powder exhibited a peak of amine N–H stretch at 3476 cm^{-1} and characteristic

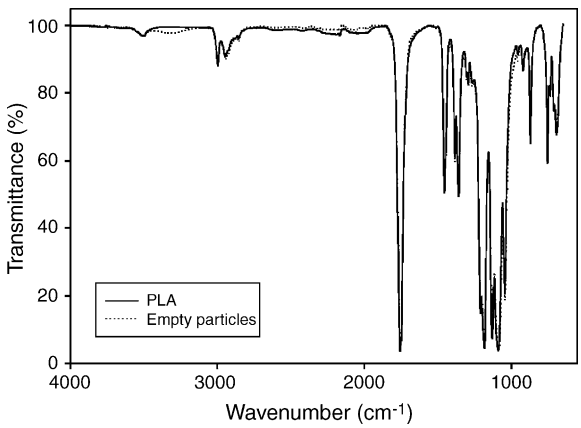

Fig. 7. IR spectra of PLA powder and empty PLA nanoparticles.

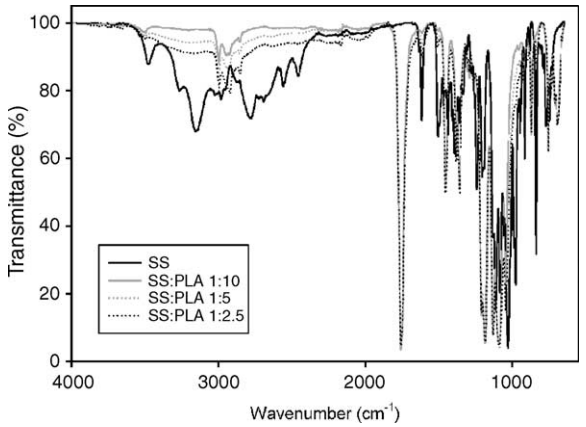

Fig. 8. IR spectra of SS powder and the SS–PLA samples.

bands of a secondary amine salt at 1617 cm^{-1} and 1507 cm^{-1} (Fig. 8). These peaks were increased, but did not change their places with increasing amounts of SS in the samples. The spectrum also showed a broad peak region of at 3400–2400 cm^{-1}, probably due to the hydroxylic groups and aromatic C–H stretching. This region was also diminished with the decreasing drug amounts. The smaller peaks can be explained by a higher relative amount of PLA in the samples. No peak shifts or new peaks appeared in the spectra, which indicate that there were no (visible) interactions between the SS and PLA.

IR spectrum of the BDP powder exhibited a broad peak at 3267 cm^{-1} and two peaks at 1658 cm^{-1} and 1615 cm^{-1}, corresponding to hydrogen-bonded hydroxyl groups, carbonyl groups and carbon double bonds, respectively (Fig. 9). In the BDP–PLA samples, these peaks were diminished and shifted to higher wavenumbers. The carbonyl peaks between 1700 cm^{-1} and 1800 cm^{-1} seen in the BDP powder spectrum seemed to be overlapped by the PLA carbonyl peak. The smaller peak sizes obviously resulted from the smaller relative amount of BDP compared to PLA. The hydroxyl peak was shifted to 3287 cm^{-1}, and the carbonyl peak and the carbon double bond peak were shifted to 1664 cm^{-1} and 1631 cm^{-1}, respectively. The hydroxyl peak around 3500 cm^{-1} in the polymer spectra was transformed into two peaks. These new peak locations corresponded to the spectrum of the monohydrate form, as presented also by Hunt and Padfield (Hunt and Padfield, 1989).

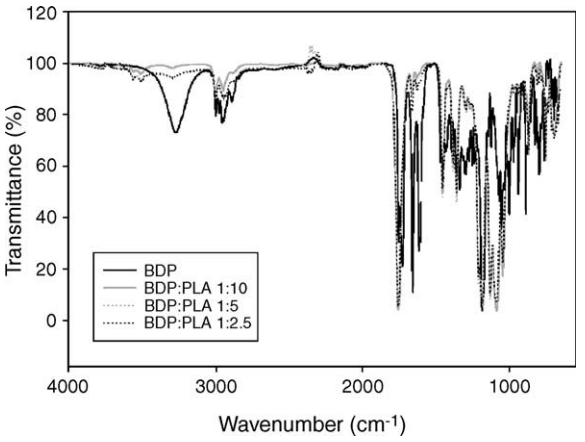

Fig. 9. IR spectra of BDP powder and the BDP–PLA samples.

3.5. Effect of modified nanoprecipitation on the size of the nanoparticles

As the nanoparticle images showed, the size distribution of SS–PLA particles was in the range of 500–900 nm, while the size of the empty particles and the BDP–PLA particles was 300–500 nm (Fig. 1). No drug crystals outside the particles could be seen in the SEM images.

In a spontaneous particle formation process, like in nanoprecipitation, the particle size obviously depends on an interplay between several variables like the organic (polymer) phase viscosity, stabilizer(s), solvent properties and the polymer properties (molecular weight, ability to precipitate and crystallize) etc. In this study, the only element that was different between the SS–PLA and the BDP–PLA nanoparticles was the drug. Thus, the reasons for the size differences may be discussed based on the previous physicochemical characterization of the nanoparticles. In the nanoprecipitation process, when the inner phase is added to the outer phase, small droplets are formed spontaneously, and they shrink as the inner phase (organic solvent) diffuses to the outer phase (Fessi et al., 1989). SS, as a water-soluble drug, is located in the aqueous droplets of the inner phase in the primary dispersion, while BDP remains in the organic phase with the polymer. If the inner phase droplets in the outer phase represent higher osmotic activity due to, for example, a water-soluble drug, flow of the outer phase into the droplets may occur (Bodmeier and McGinity, 1987). When poured to the outer phase, an osmotic pressure (concentration gradient) may have been formed between the SS-rich droplets and the aqueous outer phase. This, in turn, has created a flow of the aqueous outer phase into the droplets, which accelerates the solvent diffusion to the outer phase leading to faster precipitation of the polymer. Because of the water flow and faster precipitation, the droplet size before precipitation was bigger. This resulted to larger SS–PLA nanoparticles and more porous structure. The more porous structure provides more mobility to the polymer chains and allows water to plasticize the polymer. The plasticization enhances the crystallization of PLA (Ljungberg and Wesslén, 2002). Additionally, the rate of crystallization is increased (Martin and Avérous, 2001) Hence, the SS–PLA nanoparticles are bigger in size and the polymer is more crystalline compared to the BDP–PLA nanoparticles due to faster solvent evaporation and polymer precipitation.

4. Conclusions

Salbutamol sulphate—poly(L-lactic acid) and beclomethasone dipropionate—poly(L-lactic acid) formulations of varying drug loadings were prepared by modified nanoprecipitation. Combination of X-ray diffractometry, differential scanning calorimetry, infra red spectroscopy and scanning electron microscopy were used to clarify the physicochemical state of each drug, the PLA polymer, physical drug–polymer mixtures, and the nanoparticle formulations. Nanoprecipitation reduced the crystallinity of the polymer. Crystalline salbutamol sulphate could be detected from the samples, and the presence of the drug promoted the crystallinity of the polymer. The crystal form of beclomethasone dipropionate was changed almost completely from an anhydrate to a monohydrate during the nanoprecipitation process. The crystallinity of the polymer was higher in the salbutamol sulphate containing nanoparticles as compared to the beclomethasone dipropionate containing particles. Changes in the crystallinity of the polymer and the model drugs were seen, but no clear interactions between the polymer and the drug were detected.

Acknowledgements

Finnish Technology Agency (TEKES), Focus Inhalation Inc. (Finland) and Orion Pharma (Finland)

are acknowledged for their financial support. Electron Microscopy Unit in the Institute of Biotechnology (University of Helsinki) and Laboratory of Polymer Chemistry (University of Helsinki) are acknowledged for providing laboratory facilities and analytical equipment.

References

Benoit, J.P., Courteille, F., Thies, C., 1986. A physicochemical study of the morphology of progesterone-loaded poly(D,L-lactide) microspheres. Int. J. Pharm. 29, 95–102.

Bodmeier, R., McGinity, J.W., 1987. Polylactic acid microspheres containing quinidine base and quinidine sulphate prepared by the solvent evaporation technique. I. Methods and morphology. J. Microencapsul. 4, 279–288.

Bodmeier, R., Oh, K.H., Chen, H., 1989. The effect of the addition of low molecular weight poly(D,L-lactide) on drug release from biodegradable poly(D,L-lactide) drug delivery systems. Int. J. Pharm. 51, 1–8.

Borodkin, S., Yunker, M.H., 1970. Interaction of amine drugs with a polycarboxylic acid ion-exchange resin. J. Pharm. Sci. 59, 481–486.

Cha, Y., Pitt, C.G., 1989. The acceleration of degradation-controlled drug delivery from polyester microspheres. J. Controlled Release 8, 259–265.

Cook, P.B., Hunt, J.H., 1982. Chemical compounds. US Patent 4 364 923 (21 December).

Delgado, A., Evora, C., Llabres, M., 1996. Optimization of 7-day release (in vitro) from DL–PLA methadone microspheres. Int. J. Pharm. 134, 203–211.

Duax, W.L., Cody, V., Strong, P.D., 1981. Structure of the asthma drug beclomethasone dipropionate. Acta Cryst. B 37, 383–387.

Dubernet, C., 1995. Thermoanalysis of microspheres. Thermochim. Acta 248, 259–269.

Eerikäinen, H., Kauppinen, E.I., 2003. Preparation of polymeric nanoparticles containing corticosteroid by a novel aerosol flow reactor method. Int. J. Pharm. 263, 69–83.

El-Baseir, M.M., Phipps, M.A., Kellaway, I.W., 1997. Preparation and subsequent degradation of poly(L-lactic acid) microspheres suitable for aerosolisation: a physico-chemical study. Int. J. Pharm. 151, 145–153.

Fessi, H., Puisieux, F., Devissaguet, J.P., Ammoury, N., Benita, S., 1989. Nanocapsule formation by interfacial polymer deposition following solvent displacement. Int. J. Pharm. 55, R1–R4.

Hunt, J.H., Padfield, J.M., 1989. Micronised beclomethasone dipropionate monohydrate compositions and methods of use. US Patent 4 866 051 (12 September).

Izumikawa, S., Yoshioka, S., Aso, Y., Takeda, Y., 1991. Preparation of poly(L-lactide) microspheres of different crystalline morphology and effect of crystalline morphology on drug release rate. J. Controlled Release 15, 133–140.

Jenquin, M.R., McGinity, J., 1994. Characterization of acrylic resin matrix films and mechanisms of drug–polymer interaction. Int. J. Pharm. 101, 23–34.

Jinks, P.A., 1989. Physically modified beclomethasone dipropionate suitable for use in aerosols. US Patent 4 810 488 (7 March).

Lee, J.-H., Park, T.-G., Park, H.-K., Lee, D.-S., Lee, Y.-K., Yoon, S.-C., Nam, J.-D., 2003. Thermal and mechanical properties of poly(L-lactic acid) nanocomposite scaffold. Biomaterials 24, 2773–2778.

Li, S., Girod-Holland, S., Vert, M., 1996. Hydrolytic degradation of poly(D,L-lactic acid) in the presence of caffeine base. J. Controlled Release 40, 41–53.

Liggins, T.L., Burt, H.M., 2001. Paclitaxel loaded poly(L-lactic acid) microspheres: properties of microspheres made with low molecular weight polymers. Int. J. Pharm. 222, 19–33.

Liggins, T.L., Burt, H.M., 2004a. Paclitaxel loaded poly(L-lactic acid) (PLLA) microspheres II. The effect of processing parameters on microsphere morphology and drug release kinetics. Int. J. Pharm. 281, 103–106.

Liggins, T.L., Burt, H.M., 2004b. Paclitaxel loaded poly(l-lactic acid) microspheres 3: blending low and high molecular weight polymers to control morphology and drug release. Int. J. Pharm. 282, 61–71.

Lin, S.-Y., Chen, K.-S., Teng, H.-H., Li, M.-J., 2000. In vitro degradation and dissolution behaviours of microspheres prepared by three low molecular weight polyesters. J. Microencapsul. 17, 577–586.

Ljungberg, N., Wesslén, B., 2002. The effects of plasticizers on the dynamic mechanical and thermal properties of poly(lactic acid). J. Appl. Polym. Sci. 86, 1227–1234.

Martin, O., Avérous, L., 2001. Poly(lactic acid): plasticization and properties of biodegradable multiphase systems. Polymer 42, 6209–6219.

Martin, T.M., Bandi, N., Shulz, R., Roberts, C.B., Kompella, U.B., 2002. Preparation of budenoside-PLA microparticles using supercritical fluid precipitation technology. AAPS PharmSciTech 3 (article 18).

Mehta, R.C., Thanoo, B.C., DeLuca, P.D., 1996. Peptide containing microspheres from low molecular weight and hydrophilic poly(D,L-lactide-co-glycolide). J. Controlled Release 41, 249–257.

Miyajima, M., Koshika, A., Okada, J., Ikeda, M., Nishimura, K., 1997. Effect of polymer crystallinity on papaverine release from poly(L-lactic acid) matrix. J. Controlled Release 49, 207–215.

Nachiengtung, N., 1997. Solid state characterization of beclomethasone dipropionate solvates and polymorphs. Ph.D. Thesis, Purdue University, USA.

Peltonen, L., Koistinen, P., Karjalainen, M., Häkkinen, A., Hirvonen, J., 2002. The effect of cosolvents on the formulation of nanoparticles from low-molecular-weight poly(l)lactide. AAPS PharmSciTech. 3 (article 32).

Peltonen, L., Koistinen, P., Hirvonen, J., 2003. Preparation of nanoparticles by the nanoprecipitation of low molecular weight poly(l)lactide. S. T. P. Pharma. Sci. 13 (5), 299–304.

Ramtoola, Z., Corrigan, O.I., Bourke, E., 1991. Characterisation of biodegradable microspheres containing dehydro-isoandrosterone. Drug Dev. Ind. Pharm. 17, 1857–1873.

Ueda, M., Kreuter, J., 1997. Optimization of the preparation of loperamide-loaded poly(L-lactic acid) nanoparticles by high

pressure emulsification-solvent evaporation. J. Microencapsul. 14, 593–605.

Wang, X., Michoel, A., Van den Mooter, G., 2004. Study of the phase behavior of polyethylene glycol 6000-itraconazole solid dispersions using DSC. Int. J. Pharm. 272, 181–187.

Wichert, B., Rohdewald, P., 1990. A new method for the preparation of drug containing polylactic acid microparticles without using organic solvents. J. Controlled Release 14, 169–283.

Yasuniwa, M., Tsubakihara, S., Sugimoto, Y., Nakafuku, C., 2004. Thermal analysis of the double-melting behavior of poly(L-lactic acid). J. Polym. Sci. Part B: Polym. Phys. 42, 25–32.

Yoshioka, M., Hancock, B.C., Zografi, G., 1995. Inhibition of indomethacin crystallization in poly(vinylpyrrolidone) coprecipitates. J. Pharm. Sci. 84, 983–986.